

PREDICTION OF INITIAL STIFFNESS OF SEMIRIGID STEEL BEAM-TO-COLUMN CONNECTIONS WITH BOLTS AND ANGLES

X.G. Lin¹ and N. Hamamoto²

¹ *Assoc. Prof., Dept. of Architecture, Osaka Institute of Technology, Osaka, Japan*

² *Logistics & Automation Division, Murata Machinery, Ltd. Inuyama, Japan*

Email: lin@archi.oit.ac.jp, norifumi.hamamoto@hkt.muratec.co.jp

ABSTRACT:

The objectives of this paper are to investigate the pattern of contact between angle and column in the vicinity of bolts for semi-rigid steel beam-to-column connections with bolts and angles, and propose a mechanical model for initial stiffness reduction calculation and derive a new formula to calculate initial stiffness of the connections. In this study a nonlinear separation curve in the contact between angle and column is observed and used as foundation to develop an initial stiffness formula. Results calculated using the proposed initial stiffness formula are compared with numerical results from finite element analysis and comparison shows error within $\pm 10\%$. Results calculated using the proposed formula are also compared with some lab test results. The comparison with lab test results is not as good as comparison with numerical results because lab test instruments were chosen for ultimate strength measurement with large deformation and were not very accurate for small displacement as well as initial stiffness measurement.

KEYWORDS:

Semi-rigid connection, high strength bolt, steel frame, initial stiffness

1. INTRODUCTION

Since weld failures were observed in a lot of rigid (welded) connections of building structures during Hyogo-ken-Nambu Earthquake of Japan (on January 17, 1995), angle and split tee semi-rigid (bolted) beam-to-column connections has drawn themselves more and more attention. Semi-rigidly jointed (bolted) steel frames are more flexible than rigid jointed (welded) steel frames and provide much more energy dissipation during an earthquake. But on other hand Semi-rigidly joint steel frames will be experiencing much more deformation than rigid jointed steel frames. In the places where displacements of frames have limits, design of semi-rigidly jointed steel frames will be more challenging than design of rigid jointed steel frames. Therefore accurate calculations of displacements or initial stiffness are needed in design of semi-rigid beam-to-column connections. Regarding to how to estimate initial stiffness of semi-rigid beam-to-column connections, N.Kishi and Wai-Fan Chen (1990), A.Azizinamini (1987) have proposed a few simple formulas in last two decades. But those formulas were developed based on either a linear contact separation line between angle and column or rotationally free boundary condition so that accuracy of those formulas needs to be improved.

A series of elasto-plastic analysis of 3-D finite element models of semi-rigid connections are conducted in this work and structural deformation and separation of angle from column in the direction of width of angles are closely monitored. Based on numerical simulation results, stiffness reduction characteristics in the direction of width of top angel for semi-rigid beam-to-column connections are studied and stiffness reduction rate and a reduction coefficient are proposed. Using the same stiffness reduction rate some formulas of tension stiffness of top angle are developed and evaluated for accuracy by comparing with numerical results and lab test results.

2. STIFFNESS REDUCTION OF SEMI-RIGID CONNECTIONS

Fig. 1 illustrates a semi-rigid beam-to-column connection. In the connection, deformation of column will reduce stiffness of the connection. Stiffeners are often used to prevent and reduce deformation of column. For simplicity this study will not consider deformation of column. In a connection of beam and column with top and seat angles, deformation of top flange angle dominates deformation of the connection. Influence of seat flange

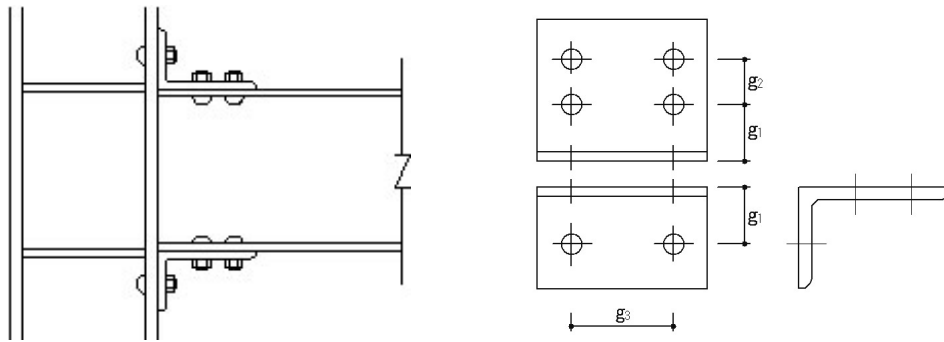


Fig. 1. Semi-rigid beam-to-column connection with top and seat flange angles

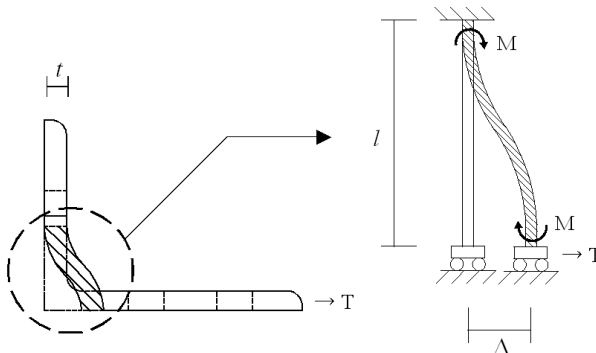


Fig. 2. Simple mechanical model

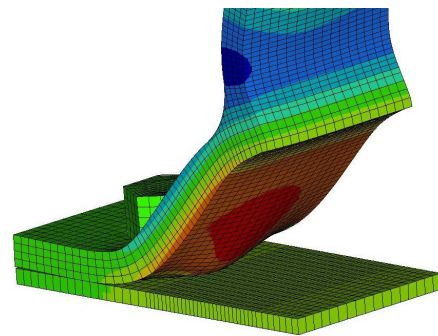


Fig. 3. Contact separation pattern

angle is relative small compared with top flange angle. To further simplify studies, only top angle tension is considered in establishing prediction formula of initial stiffness of the semi-rigid beam-to-column connection.

Fig. 2 shows the simplest modeling of top angle. This simple model has been used very often in the prediction of initial stiffness. In this model the vertical flange of angle is treated as a short beam. It is totally fixed at column bolt location and it is rotationally fixed at beam flange. This model is simple and easy to use, but it can overestimate the stiffness of the connection too much. In order to overcome this, some modifications are made such as removing rotational constraint in beam flange or releasing some constraints in column bolt location. Fig. 3 shows typical deformation in angle at column bolt location. It is easily observed that deformation in angle does not have typical characteristic of beam deformation. When beam deforms, shape of a cross section will remain the same. Here after loading shape of cross section changes and deformation in the angle is more like plate deformation. The center portion in direction of width was fixed at bolt head location while two side areas separate from column and separation spreads towards back of bolt head. In another words, fixed whole cross section is not good assumption in modeling of connection in Fig. 2. This difference is one of main reasons of stiffness calculation error. The constraint of bolt to angle is getting weaker for area away from bolt. To predict stiffness with better accuracy, this constraint weakening has to be considered.

Fig. 6 shows separation between angles and columns when the connections are loaded to yielding point. Table 1 lists detailed model data including angle size, bolt diameter and bolt pretension force. In order to study separation between angle and column and influence of bolt pretension, three FEM models with different bolt pretension forces are chosen to investigate. BA-2 is a model with standard bolt pretension force. BA-1 is a model with lower bolt pretension force and BA-3 is a model with higher bolt pretension force. Fig. 5 shows load versus displacement curves from finite element analysis of three models. FEM results indicate that insufficient pretension force will result in stiffness loss as expected and on other hand stiffness does not increase much when pretension force increases beyond standard pretension. It is also noticed that during service loading separation of angle from column stopped at bolt head location in center area but separation will keep going in two side areas beyond bolt location. A final nonlinear separation curve is formed as shown in Fig. 6. When bolt pretension is no lower than standard bolt force, the final separation curve takes 0.6 – 0.7 rad away

Table 1. Parameters of angle models

Model	Angle	Bolt	Width (mm)	g1 (mm)	g3 (mm)	Pretension (kN)
BA-1	L-30×120×12	M22	175	70	95	113
BA-2	L-30×120×12	M22	175	70	95	226
BA-3	L-30×120×12	M22	175	70	95	339

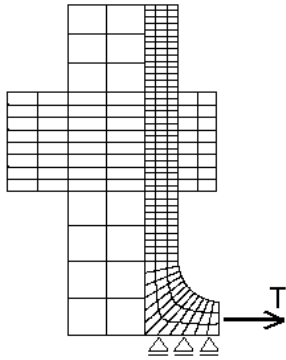


Fig. 4. Bending angle model

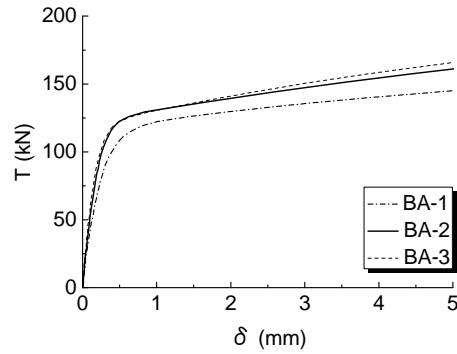
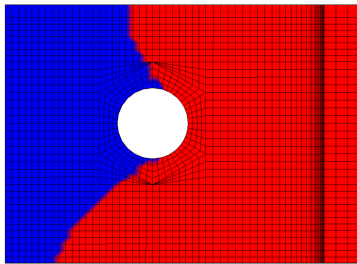
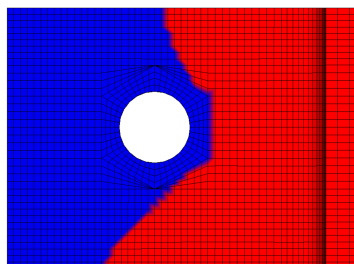


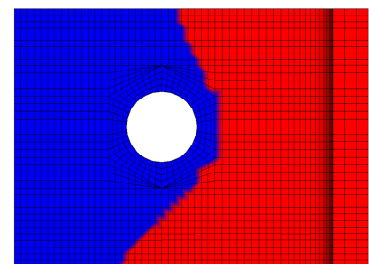
Fig. 5. Load versus displacement curves



(BA-1)



(BA-2)



(BA-3)

Fig. 6. Separation pattern in the vicinity of bolt area

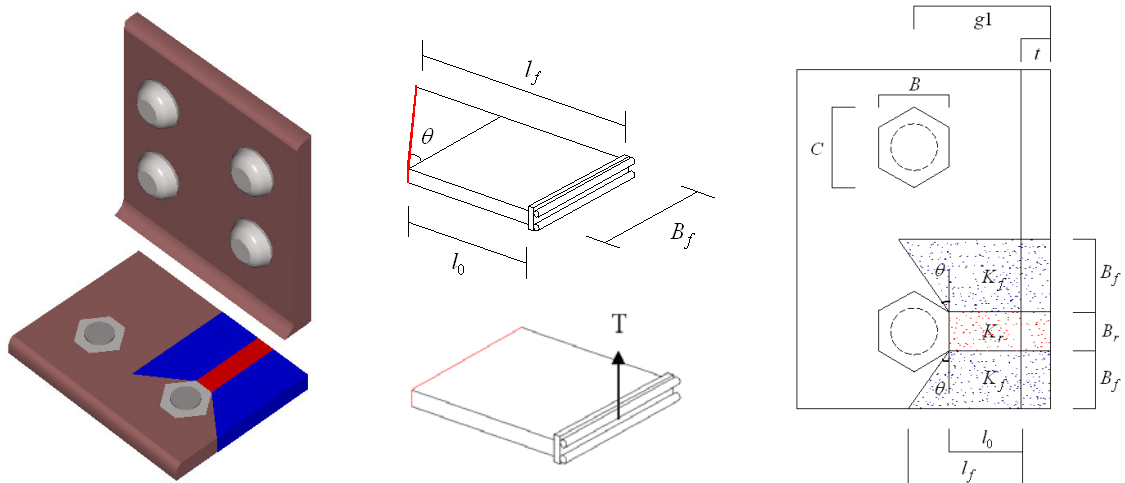


Fig. 7. Segmental beam model for top angle

from horizontal line. Additional load won't move separation curve further and separation curve will remain the same for the load range that is interested in initial stiffness study in this paper.

Based on those observations, angle will be totally fixed at separation curve when initial stiffness is calculated in this paper. Then angle is divided into many narrow beams with different lengths. Each small beam is calculated for its stiffness in the same way as to simplified model as shown in Fig. 2. This is a simple way to incorporate separation curve into initial stiffness calculation.

3. PROPOSAL OF STIFFNESS REDUCTION COEFFICIENT

Fig. 7 shows proposed mechanical model to be used in initial stiffness calculation. To have a better view, angle is turned by 90°. The left portion of angle is connected to column through two bolts. The right portion of angle is rotationally fixed. Within one bolt area, angle is divided into three segments. The center segment is red and will be called as rigid segment and two side segments are blue and will be called flexible segments. First the rigid segment is treated as a beam similar to model in Fig. 2. The rigid segment is totally fixed at bolt end and rotationally fixed at beam end. When a tensile force is applied at right end, theoretical stiffness K_r of the rigid segment due to shear deformation can be calculated by equations as follows

$$K_r = K_0 B_r, \quad K_0 = \frac{Et^3}{\ell_0^3(1+\gamma)}, \quad \gamma = 3.12 \left(\frac{t}{\ell_0} \right)^2 \quad (3.1)$$

Where K_0 is theoretical stiffness of unit width of the rigid segment, t is thickness of the angle and E is elastic modulus of steel and γ is coefficient of shear deformation. B_r and ℓ_0 are width and length of the rigid segment respectively. B_r and ℓ_0 are parameters which are to be determined based on FEM results later.

In next step the flexible segment will be treated as a collection of many narrow beams with small width. Let x represent transverse distance of any narrow beam from the rigid segment and length of the narrow beam is $\ell = \ell_0 + \theta \cdot x$, integration of the stiffness of the flexible segment yields a equation for total stiffness as follows

$$K_f = \int_0^{B_f} \frac{Et^3}{(\ell_0 + \theta \cdot x)[(\ell_0 + \theta \cdot x)^2 + \gamma \cdot \ell_0^2]} dx = \frac{Et^3}{2\gamma \cdot \ell_0^2 \theta} \ln \frac{\ell_f^2(1+\gamma)}{\ell_f^2 + \gamma \cdot \ell_0^2} \quad (3.2)$$

Where B_f is the width of the flexible segment, ℓ_f is the length of outer side of the flexible segment and θ is the angle of separation curve. Here we are going to introduce concept of stiffness reduction coefficient. Equation (3.2) is rearranged to equation as follows

$$K_f = \alpha \cdot K_0 B_f, \quad \alpha = \frac{(1+\gamma)}{2\gamma(\beta-1)} \ln \frac{\beta^2(1+\gamma)}{\beta^2 + \gamma}, \quad \beta = \frac{\ell_f}{\ell_0} = 1 + \frac{\theta \cdot B_f}{\ell_0} \quad (3.3)$$

Where α is a stiffness reduction coefficient, which is a stiffness ratio between the rigid segment and the flexible segment with unit width. β is a length ratio of two sides of the flexible segment. The stiffness reduction coefficient is complicated and hard to calculate. Considering range of β and γ in most applications ($\beta=1.0-3.0$, $\gamma=0.07-0.7$), calculation for α can be simplified as

$$\alpha = \beta^{\left(\frac{\gamma}{3}-1.4\right)} \quad (3.4)$$

It can be seen that equation (3.4) is much simpler and easier to use. Fig. 8 shows the relationship between width B_f and stiffness reduction coefficient α . The wider the width, the weaker bolt constraint is to of-plane deformation of angle. The stiffness can be reduced by half when width is very wide. In the plot in Fig. 8 the curve of stiffness reduction coefficient from original equation and curve of stiffness reduction coefficient from simplified equation are compared. This comparison indicates simplification does not introduce noticeable error.

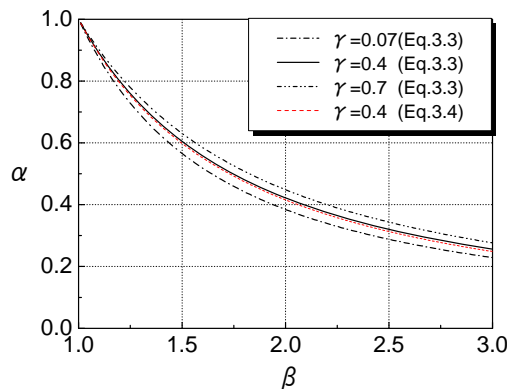


Fig. 8. Reduction coefficient in the direction of width of angle

In order to confirm the accuracy of stiffness reduction coefficient as well as to choose values for parameters B_r and l_0 , some finite element analyses are conducted using a plate model shown in Fig. 9. Data of the length and the width of plates are given in Table 2. The length in the table is the distance from bolt head to rigid end. The left side of model is bolted to flange of column and the right side of model is connected to rigid body. Rigid body has rotationally fixed constraint. The plate is divided into three segments. Finite element model is loaded by displacement and three segments are all subject to the same displacement. Steel properties are taken from test results of JIS SS400 and elasto-plastic behavior of steel is considered in finite element analysis.

Fig. 10 shows the load-displacement curves from numerical analysis. It is difficult to define a slope even at the beginning of loading. Due to contact separation and local plastic deformation, stiffness goes down when load is increasing. After steel yielding stiffness goes down rapidly. To give clear definition for initial stiffness, a point is chosen when its tangent stiffness is reduced to half of its secant stiffness. At this point the secant stiffness is defined as initial stiffness. It is believed that steel plastic deformation has little influence to stiffness up to this point. Initial stiffness results from FEM are listed in Table 3. Stiffness prediction using equations (3.1) and (3.4) are also included in Table 3. Before carrying out finite element analysis of those models, a simple analysis of a cantilever beam is tested for comparison of accuracy of calculation using theoretical formula and finite element model. It is concluded that finite element analysis produces stiffness 9% higher than theoretical result. Therefore, comparison target in Table 3 is set to be 0.91.

Table 2. Parameters of plate models

Model	Thickness (mm)	Length (mm)	Bolt	B_r (mm)	B_{r1} (mm)	B_{r2} (mm)
BP-1	12	42	M20	18.5	25.8	30.7
BP-2	12	42	M20	18.5	25.8	51.6
BP-3	12	56	M20	18.5	25.8	30.7

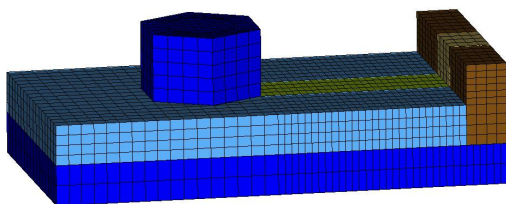


Fig. 9. Bending plate model

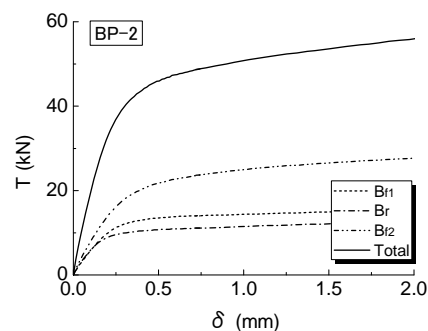


Fig. 10. Load versus displacement curves

Table 3. Comparison of predicted initial stiffness with FEM numerical results

Model	ℓ_0 (mm)	FEM (kN/mm)				Predicted (kN/mm)				R= Predicted / FEM			
		K _r	K _{f1}	K _{f2}	K _{total}	K _r	K _{f1}	K _{f2}	K _{total}	R _r	R _{f1}	R _{f2}	R _{total}
BP-1	50.4	486	453	510	1444	435	412	462	1309	0.895	0.909	0.906	0.907
BP-2	50.4	486	453	596	1521	435	412	612	1459	0.895	0.909	1.027	0.959
BP-3	64.4	227	248	272	754	221	225	255	701	0.974	0.907	0.938	0.930

In prediction of initial stiffness, angle of separation curve is set $\theta = 0.65rad$. The width of the rigid segment is taken as $B_r = C/2$. C is the size of bolt head as shown in Fig. 7. When value of parameter ℓ_0 is decided, in-plate deformation through thickness of plate is considered, separation curve is set at a distance of 0.7 times of thickness behind the front face of bolt. It can be seen that comparison between predicted stiffness and FEM stiffness of all three segments do not show much difference. It is also noticed that the wider the width is and higher the difference is. But difference between the predicted and FEM results are close to 0.91 in term of total stiffness. It is concluded that equations (3.1) & (3.4) can be used to predict initial stiffness from finite element analysis.

4. PREDICTION OF TENSION STIFFNESS OF TOP ANGLE

Design of a tension test specimen is illustrated in Fig. 11. A specimen is made of 4 angles of same dimension, two tension plates of same dimension and one compression plate. Tension plate could be viewed as flanges of beam in semi-rigid beam-to-column connections. Compression plate restrains the deformation of angles. An Amsler type universal testing machine is employed to apply tensile load to specimen. All specimens are loaded to failure, in which either angle or bolt fractured.

All angles are made of JIS SS400 steel. Four different thicknesses are 9 mm, 12 mm, 15 mm and 20 mm. Two types of high strength bolts are M20 and M22 of class F10T. All 15 specimen tested are listed in Table 4. In those tests test equipment is chosen to measure the largest deformation

when specimens reach their ultimate strength so that test reading is not very accurate when displacement is small. The target of this paper is to predict initial stiffness instead of stiffness when steel yields. So about half of test results are not valid to give required stiffness data. To overcome this, finite element analyses are performed on all tension specimens. Fig. 12 shows some of those results. Those predicted stiffness will be compared with both test results and FEM results.

Some difference exists between semi-rigid connections and pure plate model. Angle connection model in Fig. 1 and Fig.11 does not have rigid body as shown in Fig. 9 and has only plate at other side (beam or tension plate side). Also this plate will deform as elastic deformable body and lead to stiffness loss. The plate is connected to beam through bolt and couldn't possess non-rotational boundary condition. On other hand, fillet in angle

Table 4. Parameters of tension test specimens

Specimen	Angle	Bolt	Width (mm)	g1 (mm)	g3 (mm)
A20-9	L-150×100×9	M20	150	50	90
A20-12	L-150×100×12	M20	150	50	90
B20-9	L-150×100×9	M20	150	60	90
B20-12	L-150×100×12	M20	150	60	90
B22-12	L-150×100×12	M22	150	60	90
C20-12	L-175×120×12	M20	150	70	80
C20-15	L-175×120×15	M20	150	70	80
C22-12-1	L-175×120×12	M22	150	70	80
C22-12-2	L-175×120×12	M22	175	70	95
C22-12-3	L-175×120×12	M22	175	70	115
C22-15	L-175×120×15	M22	150	70	80
D22-12	L-175×130×12	M22	175	80	95
D22-20	L-190×130×20	M22	150	80	80
E22-15	L-175×120×15	M22	175	65	95
F22-20	L-190×130×20	M22	150	90	80

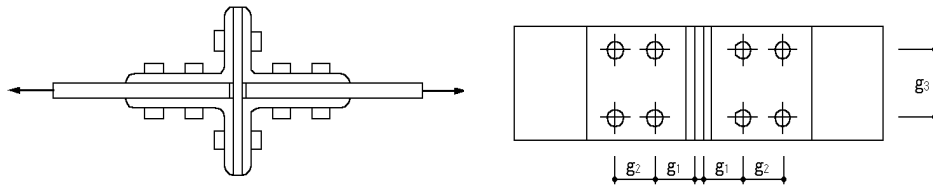


Fig. 11. Tension test specimen

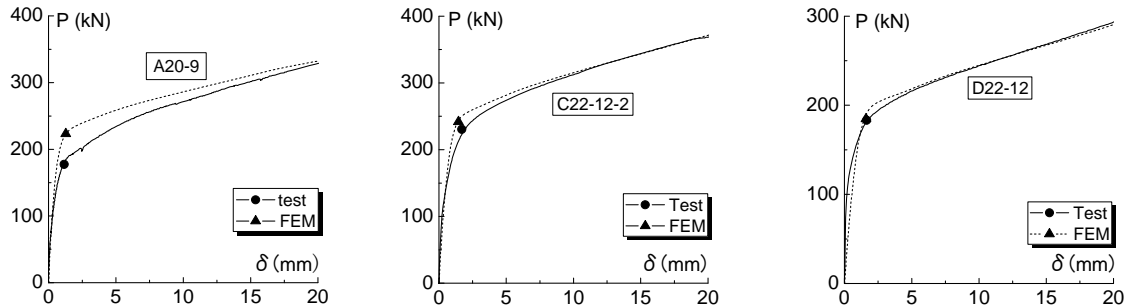


Fig. 12. Comparison between test results and FEM numerical results

Table 5. Comparison of predicted initial stiffness with FEM and lab test results

Specimen	Test (kN/mm)	FEM (kN/mm)	Predicted (kN/mm)	No.	Specimen	Test (kN/mm)	FEM (kN/mm)	Predicted (kN/mm)	No.
A20-9	241.3	285.4	271.7	1	C22-12-2	----	245.1	231.6	9
A20-12	----	600.6	603.2	2	C22-12-3	246.6	231.4	225.0	10
B20-9	120.6	144.5	139.0	3	C22-15	----	410.3	402.3	11
B20-12	339.0	308.3	318.3	4	D22-12	----	151.6	145.1	12
B22-12	282.8	374.3	368.2	5	D22-20	----	550.0	568.0	13
C20-12	----	202.6	188.5	6	E22-15	469.8	533.5	562.4	14
C20-15	----	349.4	356.7	7	F22-20	266.7	351.5	386.6	15
C22-12-1	----	236.2	213.4	8					

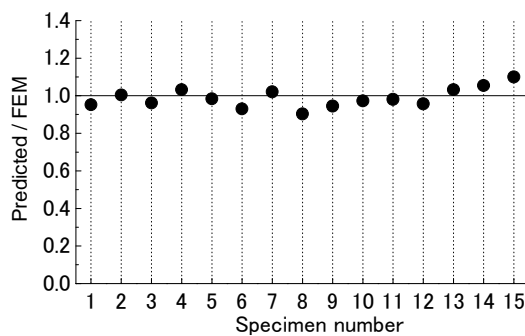


Fig. 13. Comparison of predicted initial stiffness with FEM numerical results

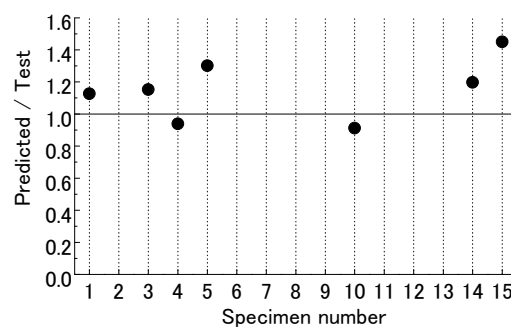


Fig. 14. Comparison of predicted initial stiffness with lab test results

increases stiffness. In order to understand those factors, some FEM are carried out to study influence of those factors. FEM results show that stiffness increase from fillet cancels stiffness loss due to elastic deformation of plate. But stiffness will be reduced by 70-80% because of rotation in bolt connection. Based on those observations tension stiffness formula is proposed as

$$K = 0.72K_0(B_r + \alpha_1 B_{f1} + \alpha_2 B_{f2}) \quad (4.1)$$

In the equations of stiffness reduction coefficient α_1 and α_2 , the base length ℓ_0 is $\ell_0 = g_1 - t - 0.5B + 0.7t = g_1 - 0.3t - 0.5B$. B is the size of bolt head as shown in Fig. 7. Table 5 shows comparison of test stiffness and FEM stiffness as well as predicted stiffness from equation in this paper. Fig. 13 shows comparison of predicted stiffness and FEM stiffness with difference within $\pm 10\%$. Most of specimens only show difference within $\pm 5\%$. Fig.14 shows comparison of predicted stiffness and test stiffness with difference larger than in Fig. 13. It is believed that less accurate stiffness measurement in lab test is responsible for larger error.

5. CONCLUDING REMARKS

A series of FEM elasto-plastic analysis was conducted in order to understand contact pattern around bolt hole between angle and column. It is observed that angle starts separating from column pretty soon after loading starts. Separation reaches bolt hole even when load is low and stops progressing in front side of bolt when load increases. But on lateral sides of bolt separation will keep spreading and forms a nonlinear separation boundary between angle and column. Using those observations, a concept of nonlinear separation curve is proposed and used to create mechanical model and propose some formulas for stiffness reduction coefficient. Stiffness reduction coefficient formulas are verified against FEM results and used in developing a formula for tension stiffness of top flange angle. 15 specimen tested by author are calculated for initial tension stiffness using proposed initial stiffness formula and modeled for finite element analysis. Finally all these stiffness results including initial stiffness prediction using formula proposed in this paper, and stiffness results from finite element analysis as well as lab test results are compared. Initial stiffness calculated using stiffness formula proposed in this paper shows very good correlation with numerical results from finite element analysis. The largest difference between them is about $\pm 10\%$. Most of cases only show a few percent differences. But both calculated initial stiffness using formula proposed in this paper and initial stiffness from finite element analysis do show some difference compared with lab test results. It is believed that displacement recorded from lab tests are not accurate because lab test were designed for ultimate strength measurement and equipment are not accurate in measuring small displacement before steel yields, which is the interested range for initial stiffness study.

REFERENCES

- Kishi, N. and Chen, W.F., (1990). Moment-rotation relations of semirigid connections with angles, *Journal of Structural Engineering*, **116:7**, 1813-1834.
- Ohi, K., Lin, X.G. and Nishida, A., (1996). Sub-structuring pseudo-dynamic test on semi-rigidly jointed steel frames, *Proceedings of the 11th World Conference on Earthquake Engineering*, Mexico, Paper No. 410.
- Azizinamini, A., Bordburn, J.H. and Radzimirski, J.B., (1987). Initial Stiffness of Semi-rigid Steel Beam-to-Column Connections, *Journal of Constructional Steel Research*, **8**, 71-90.
- Lin, X.G. and SUGIMOTO, H., (2004). Experimental Study on Inelastic Behavior and Ultimate Strength of Steel Beam-to-Column Connections with Bolts and Angles, *Proceedings of the 13th World Conference on Earthquake Engineering*, Canada, Paper No. 1673.
- Tanuma, Y., and Hashimoto, K., (1999). Moment-rotation behaviour of semirigid connections with angles, *Journal of Structural and Construction Engineering*, **515**, 123-130.
- Tanaka, H., and Tanaka, A., (1975). Design formulas for the strength of t-stub connection, *Steel Construction Engineering*, **11:120**, 5-10.